Supplementary Materials for

Staphylococcus aureus and *S. epidermidis* strain diversity underlying human atopic dermatitis

Allyson L. Byrd[1,2,3], Clay Deming[1], Sara K.B. Cassidy[1], Oliver J. Harrison[3], Weng-Ian Ng[1], Sean Conlan[1], NISC Comparative Sequencing Program[4], Yasmine Belkaid[3,5], Julia A. Segre[1*], Heidi H. Kong[6*]

correspondence to: jsegre@mail.nih.gov; konghe@mail.nih.gov

This PDF file includes:

Materials and Methods

Experimental design

Patients with AD and similarly aged healthy controls were recruited from the Washington DC metropolitan region, USA, between June 2012 and March 2015, to participate in a natural history study approved by the Institutional Review Board of National Human Genome Research Institute (http://www.clinicaltrials.gov/ct2/show/NCT00605878).

Eligibility criteria included age 2-18 years, moderate-to-severe disease, presence of ≥1 affected antecubital crease (inner elbow) or popliteal crease (behind the knee) at enrollment, and >3 weeks off of systemic antibiotics and corticosteroids. Patients were diagnosed with AD based on the UK Working Party definition (*1*). Disease severity was measured by the objective SCORAD as assessed by a board-certified dermatologist (HHK). At each clinical visit, objective SCORAD was used to determine study eligibility and disease status (*2-4*). Moderate-to-severe disease was defined by objective SCORAD ≥ 15 (range 0-83) (*4*).

For all subjects, exclusion criteria included receiving investigational new treatments, ultraviolet light therapy, monoclonal antibodies, systemic immunosuppressants within 7 days or five half-lives (taking the longer time period) of skin sampling, and clinically apparent underlying immunodeficiency. AD patients were also excluded if they took systemic antibiotics during the preceding three weeks (except for the post-flare timepoint). For healthy controls, additional exclusion criteria included current or prior chronic skin disease such as AD or psoriasis; asthma, via International Study of Asthma and Allergies in Childhood questionnaire (*5*); other chronic medical conditions; and use of systemic antibiotics in the preceding 6 months.

Written consent was obtained from parents or guardians of all participating children. At all clinic visits, complete medical and medication history and skin examination was performed. To standardize skin sampling and optimize microbial load, no bathing, shampooing or emollients were permitted within 24 hours of sample collection. AD patients were sampled at three timepoints (baseline, flare, and post-flare) to capture the different stages of the chronic relapsing, remitting skin disease. Healthy controls were matched based on Tanner stage, which can be used to define an individual's stage of puberty based on physical examination. Unlike chronological age which does not necessarily correspond with a defined stage in sexual maturation, Tanner staging of sexual maturity can provide a phenotypic assessment of the physiologic age of an individual.

For AD patients in this study, baseline was defined as usual and stable disease state and ability to tolerate ≥7 days without topical AD treatments to intended sample sites and >2 weeks off both oral antibiotics and corticosteroids. The skin preparation regimen of 7 days without topical steroids or topical antimicrobial regimens prior to skin sampling was used to minimize the potential confounding effects of topical therapies on skin microbiota (*6*). Five of the 11 patients successfully reached a baseline state during the course of this study; the remaining patients required reinitiation of treatment due to clinical worsening of skin disease. For flare timepoints: when skin disease worsening was apparent, patients were instructed to promptly contact the research team for evaluation. Flare was defined as acute exacerbation of the disease on any skin site without use of

skin-directed antibiotic or anti-inflammation treatments in preceding seven days and prior to initiation of intensified AD treatment. Post-flare was defined as 10-14 days after the initiation of intensified skin-directed AD treatment (not systemic or topical antibiotics and sampled at least 24 hours since last topical medication or emollient use. Recommendations for intensified AD treatment were skin-directed and included the following based on the patient's typical regimen: dilute bleach baths (0.25 cup of 6% bleach into bath half filled with water for a final concentrations of 0.0005%) two to four times per week, regular use of topical steroids twice daily, and bland emollients at least twice daily.

Seven sites were sampled bilaterally to represent the sites of disease predilection (antecubital creases and popliteal creases) and the different physiological characteristics of the skin (fig. S1): dry (volar forearm/inner forearm), moist (antecubital crease, inguinal crease, popliteal crease), and sebaceous (glabella/central forehead, retroauricular crease/behind the ear, occiput/back of lower scalp). To obtain sufficient DNA for metagenomic sequencing, sites were sampled using a swab-scrape-swab procedure (*7*). All samples were stored in lysis buffer at -80C until DNA extraction. In addition to sequencing, swabs were taken from the antecubital crease, retroauricular crease, and the nares for culture analysis (details below).

DNA extraction and sequencing of metagenomic samples

Procedures for library generation, sequencing, and processing of longitudinal samples were as described previously (*7*). Briefly, metagenomic DNA was prepared for sequencing using the Nextera DNA Library Prep Kit (Illumina) per manufacturer's instructions with the exception of increasing from 6 to 10 PCR cycles and increasing the AMPure XP Beads clean-up volume from 30uL to 50uL. Libraries were sequenced on an Illumina HiSeq at the NIH Intramural Sequencing Center to a target of 15 to 50 million clusters of 2 x 125bp reads. In total, for 18 individuals (11 patients and 7 controls), sampled at 7 body sites at different stages of disease for AD patients we obtained 422 samples and 2.26 trillon reads (191 Gb) of non-human, quality- filtered paired-end and singleton reads (median 2.4 million reads (.21 Gb) per sample). For sample processing, human reads were removed based on mapping to the hg19 + hg19 rRNA human reference genome, bases with quality scores below 20 were trimmed, and remaining reads less than 50bp were removed, as well as singletons. To reduce computational burden, post quality control, samples with >20 million reads were subsampled to 10 million paired end reads.

Variant calling of FLG gene in metagenomic samples

Reads that mapped to the FLG locus were extracted from the eland-aligned (hg19) metagenomic sequencing data using samtools (coordinates=chr1:152,274,651-152,297,679). The number of reads extracted from each of the 11 AD subject's aggregate metagenomic sequencing data ranged from 2,940-23,039 reads, corresponding to 16-126x coverage of the FLG gene. Variants were called using the Most Probable Genotype (MPG) software (*8*).

Taxonomic classification of skin species and diversity estimates

Microbial reads were assigned taxonomic classifications as previously described (*7*). Included in the microbial reference genome database are 2,342 bacteria, 389 fungal,

1,375 viral, and 67 archaeal genomes. In addition, a staphylococcus database was compiled from 315 complete and draft genomes from the National Center for Biological Information (NCBI, http://www.ncbi.nlm.nih.gov) as of October 2014. Nonhuman reads were separately mapped to both genome collections using bowtie2's –very-sensitive parameter with –k 10 to retrieve the top 10 hits (*9*). The resulting alignment files were processed with Pathoscope v1.0 (*10*) to assign multiply mapped reads to their most likely genome of origin. Read hit counts were then normalized by genome and scaled to sum to one. Coverages of each output genome were calculated using genomeCoverageBed in the the Bedtools suite (*11*). To reduce the effects of spurious classifications from low abundance organisms, only species with ≥ 1 percent coverage of the genome were considered (*7*). For the multi-kingdom database, the Shannon diversity index was used for diversity comparisons. To reduce the potential for erroneous strain-calling, for species with multiple strains in the database, hits from all strains were combined to yield a total relative abundance for the species.

Strain tracking of *S. aureus* and *S. epidermidis*

Strain tracking of the dominant flare species *Staphylococcus aureus* and *Staphyloccocus epidermidis* was performed as previously described (*7*). Briefly, reference databases for *S. aureus* and *S. epidermidis* were compiled from all complete and draft genomes available on NCBI, 215 and 61, respectively. For both species, whole genome alignment, with nucmer (*12*), was then used to identify the "core" region shared between all sequenced strains. SNVs identified in these core regions were subsequently used to generate dendograms with PhyML 3.0. Based on the dendograms, we grouped strains into subtypes or clades, 34 for *S. aureus* and 14 for *S. epidermidis.* Due to redundancy in many of the *S. aureus* draft genomes, a consolidated tree composed of all 42 complete genomes and 19 representative draft genomes was generated for visualization purposes (Fig. 3A). For strain-tracking to avoid noise from other staphylococcal species, metagenomic reads were first filtered against the staphylococcus database minus the species being strain-tracked (--very-sensitive, -score-min L,-0.6,0.006). The remaining reads were then mapped to each species database with bowtie2 (--very-sensitive, -score-min L,- 0.6,0.006, -k number of genomes)(*9*) with zero tolerance for mismatches. The resulting alignment file was then processed with Pathoscope (-theta_prior 10 x 10^88) (*10*) to deconvolute multiple mapping reads. Accuracy of this strain- tracking approach was previously validated with extensive simulations (*13*).

Identification of SNVs in the *S. aureus* core

To achieve sufficient coverage for SNV analysis, all samples for each *S. aureus*-predominant patient were combined. For SNV analysis as described previously (*14*), metagenomic reads were mapped against the *S.aureus* core genome using bowtie2 (--very-sensitive). The resulting alignment file was sorted by samtools and then processed with GATK's IndelRealigner (*15*). The corrected alignment file was analyzed with samtools and bcftools to identify possible variants (samtools mpileup -uD -q30 -Q30, bcftools view -Abvcg, vcfutils.pl varFilter -D99percentileofcoverage -d4 -1 .00001 -4 .00001). Custom scripts were then used to filter possible variants based on criteria described in (*16*). Briefly, an alternate allele was only considered if it was supported by >2 reads with a minimum mapping quality of 30, had an allele frequency >3%, and fewer than 20% of reads supporting the SNV also mapped to an indel. Due to limited numbers

of reads in some of the patients, SNVs were detected in subsamples of 350,000 reads for each patient.

Patient isolate collection, genome sequencing, and annotation

Skin and nasal cultures were obtained with Catch-all Collection Swabs (Epicentre) pre-moistened with Fastidious Broth (Remel), placed in 2.0ml Fastidious Broth supplemented with 10% glycerol, and frozen at -80°C. Swabs were thawed, vortexed, serial diluted, and plated on Tryptic Soy Agar with 5% Sheep Blood (Remel). After overnight incubation at 37°C, colonies were picked and stored in LB with 20% glycerol. Colonies were screened by PCR for *S. aureus* using Nuc1 (5′-GCGATTGATGGTGATACGGTT-3′) and Nuc 2 (5′ AGCCAAGCCTTGACGAACTAAAGC-3′), or *S. epidermidis* using Se705-1 (5'-ATCAAAAAGTTGGCGAACCTTTTCA-3') and Se705-2 (5'-CAAAAGAGCGTGGAGAAAAGTATCA-3') as previously described (*17*) (*18*). Individual colonies were then streaked on blood agar for two passages. Isolates were grown overnight in Tryptic Soy Broth at 37C, pelleted with centrifugation, and genomic DNA was extracted using the Promega Maxwell Tissue DNA Kit with the addition of Readylyse Lysozyme Solution (Epicentre) and Lysostaphin (Sigma). DNA was treated with RNase, re-purified with the Genomic DNA Clean and Concentrator Kit (Zymo), and quantified using a Nanodrop spectrophotometer and Qubit (ThermoFisher). 1.0ng of bacterial DNA was used as input into the Nextera XT Sample prep kit (Illumina) as suggested by manufacturer.

Nextera libraries were generated from the genomic DNA and sequenced using a paired-end 300-base dual index run on an Illumina MiSeq to generate 1 million to 2 million read pairs per library for ~80x genome coverage. Reads for each isolate were assembled with MaSuRCA (version 2.2.1) (*19*), SPAdes (version 3.6.0), or SPAdes (version 3.6.0) (*20*) plus Pilon (version 1.13) (*21*) correction. Best k-mer length estimates on paired-end reads were evaluated using KmerGenie (version 1.6300)(*22*) and utilized in running the MaSuRCA assembler for each genome. The SPAdes assembler was run using K-mer values of 21, 33, 55, 77, 99, and 127. Contigs >= 500 nt were retained. For comparative genomic analysis, genome annotation was done using the GS Analysis Engine (http://ae.igs.umaryland.edu/cgi/index.cgi, (*23*)). For upload to NCBI, genome annotation was done using the NCBI Prokaryotic Genomes Automatic Annotation Pipeline (PGAAP: http://www.ncbi.nlm.nih.gov/genome/annotation_prok/).

Methicillin Resistance

Glycerol stocks from clinical isolates as well as control strains (ATCC:BA1556; ATCC:29213) were plated overnight on blood agar. Individual colonies were then plated on Mannitol Salt Agar (Remel) and Mannitol Salt Agar with Oxacillin (Remel). Plates were scored for Mannitol fermentation and growth or no growth at 35°C for 24hrs.

To verify these results with a Cefoxitin Disk assay, individual colonies were picked and completely resuspended in SOC Broth. The suspension was plated on Mueller-Hinton Agar (Remel) and allowed to dry 5 minutes. One 30 µg Cefoxitin Disk (BD) was placed on the plate and incubated at 35°C for 24hr. Zones of inhibition were measured and scored as described (*24*). Briefly, *S. aureus* was scored as susceptible

≥22mm and resistant ≤21mm. *S. epidermidis* was scored as susceptible ≥25mm and resistant ≤24mm.

Pangenome analysis of *S. aureus* assemblies

To identify the functional capacity of *S. aureus* isolates from our more severe patients we followed a procedure similar to that in (*14*). The IGS Analysis Engine was used for structural and functional annotation of the sequences. (http://ae.igs.umaryland.edu/cgi/index.cgi, (*23*)). Manatee was used to view annotations (http://manatee.sourceforge.net/). Protein sequences were then clustered into non-redundant orthologs with usearch (- cluster_fast -id 0.60 -centroids) (*25*). Singletons, clusters composed of a single sequence, were then filtered based on previously established criteria (*26*). Briefly, singletons were excluded if they 1) were shorter than 50 amino acids, 2) were flagged as low complexity by Prinseq (*27*), or 3) had a blast hit to a cluster at -e 1e-10. In the end, 3,148 unique clusters of genes were identified. These gene clusters were then annotated by BLASTp against the KEGG database. Distribution of genes between the 6 *S. aureus* assemblies was visualized with jvenn (*28*).

Mice

C57BL/6 specific pathogen free (SPF) mice were purchased from Taconic Farms. All mice were bred and maintained under pathogen-free conditions at an American Association for the Accreditation of Laboratory Animal Care (AAALAC)-accredited animal facility at the NHGRI and housed in accordance with the procedures outlined in the Guide for the Care and Use of Laboratory Animals. All experiments were performed at the NHGRI under an animal study proposal approved by the NHGRI Animal Care and Use Committee. Female mice between 6 and 12 weeks of age were used for each experiment. In general, each mouse of the different experimental groups is reported. Exclusion criteria such as inadequate staining or low cell yield due to technical problems were pre-determined. Animals were assigned randomly to experimental groups.

Topical association

Topical association of mice was based on (*29*). 10 *S. aureus* strains AD04.E17, AD06.E13, AD03.A2, AD01.F1, AD11.B1, AD11.E17, AD07.B2, HC.B1, USA300 FPR3757 and 3 *S. epidermidis* strains AD05.A29, AD10.A30, and AD01.B, isolated from AD patients, controls (HC.B1), or ATCC (USA300), were cultured in tryptic soy broth at 37°C for 18h. Before topical application, bacteria were enumerated by assessing colony-forming units using traditional bacteriology techniques and by measuring optical density (OD) at 600 nm using a spectrophotometer.

For topical association, a sterile epicenter Catch-All swab was moistened in liquid culture of the bacteria and then rubbed against the ears of mice until they became visually moist. Topical association was repeated every other day four times. For each experiment, 18h cultures were normalized using OD600 to achieve similar bacterial density (approximately 10^8 c.f.u. per ml). Mice were euthanized 8 days after the first topical association with bacteria.

Tissue processing

Cells from the ear pinnae of mice were isolated as previously described (*30*). Briefly, ears were excised and separated into dorsal and ventral sheets. Tissue samples

were digested in RPMI 1640 containing 2 mM L-glutamine, 1 mM sodium pyruvate and nonessential amino acids, 20 mM HEPES, 100 U/ml penicillin, 100 mg/ml streptomycin, 50 mM β-mercaptoethanol, and 0.25 mg/ml Liberase purified enzyme blend (Roche Diagnostic Corp.) and incubated for 1 hour 45 minutes at 37°C in 5% CO2. Digested skin sheets were homogenized using the Medicon/Medimachine tissue homogenizer system (Becton Dickinson).

In vitro restimulation

For detection of basal cytokine potential, single-cell suspensions from ear tissue were cultured directly ex vivo in a 96-well U-bottom plate in complete medium (RPMI 1640 supplemented with 10% fetal bovine serum (FBS), 2 mM L-glutamine, 1 mM sodium pyruvate and nonessential amino acids, 20 mM HEPES, 100 U/ml penicillin, 100 mg/ml streptomycin, 50 mM β-mercaptoethanol) and stimulated with 50 ng/ml phorbol myristate acetate (PMA) (Sigma-Aldrich) and 5 mg/ml (mouse) ionomycin (Sigma-Aldrich) in the presence of brefeldin A (GolgiPlug, BD Biosciences) for 2.5 h at 37°C in 5% CO_2. After stimulation, cells were assessed for intracellular cytokine production as described below.

Flow cytometric analysis

Murine single-cell suspensions were incubated with fluorochrome-conjugated antibodies against surface markers CD4 (clone RM4-5), CD8β (eBioH35-17.2), CD11b (M1/70), CD11c (N418 or HL3), CD19 (6D5), CD45.2 (104), CD49b (DX5), CD64 (X54-5/7.1), Ly6G (1A8), MHCII (M5/114.15.2), NK1.1 (PK136), TCRγδ (GL3), TCRβ (H57-597), and/or SiglecF (E50-2440) in Hank's buffered salt solution (HBSS) for 20 min at 4°C and then washed. LIVE/DEAD Fixable Blue Dead Cell Stain Kit (Invitrogen Life Technologies) was used to exclude dead cells. Cells were then fixed for 30 min at 4°C using the eBioscience fixation kit and washed twice with corresponding permeabilization buffer. For simultaneous Foxp3 and intracellular cytokine staining, cells were stained with fluorochrome-conjugated antibodies against Foxp3 (FJK-16 s), IFN-γ (XMG- 1.2), IL-13 (eBio-13A) and IL-17A (eBio17B7) in permeabilization buffer (eBioscience) for 1 hr at 4°C. Each staining was performed in the presence of purified anti-mouse CD16/32 (93), 0.2 mg/ml purified rat IgG and 1 mg/ml of normal mouse serum (Jackson Immunoresearch). All antibodies were purchased from eBioscience, Biolegend, or BD Biosciences. Cell acquisition was performed on a Fortessa flow cytometer using FACSDiVa software (BD Biosciences) and data were analyzed using FlowJo software (TreeStar).

Histology

Mice were euthanized on day 8 after topical application of the AD patient isolates. TSB associated mice were used as controls. The ears from each mouse were removed and fixed in PBS containing 10% formalin. Paraffin-embedded sections were cut at 0.5 mm, stained with haematoxylin and eosin and examined histologically.

Statistics

All statistical analyses were performed in R and the majority of graphs generated with ggplot2 (*31*). Data are represented as mean ± standard error of the mean unless otherwise indicated. As disease severity differed minimally from left to right symmetric

sites, left and right values were averaged in relative abundance plots and prior to statistical comparisons. AcPc indicates the mean of values from samples of the antecubital and popliteal crease for each individual (post-averaging of left and right symmetric sites). To avoid repeated measures when all sites were considered, samples belonging to an individual were averaged before statistical comparisons between timepoints when using summary metrics such as means, diversity, or theta indices.

Pearson correlations of non-zero values were used for all partial correlations adjusting for disease state (pcor.test in R package ppcor). For all boxplots, center lines represent the median and edges the first and third quartiles. The nonparametric Wilcoxon rank-sum test was used to determine statistically significant differences between populations (wilcox.test in R). Where indicated, within-subject analysis was performed with option "paired=T" in wilcox.test. All *p*-values were adjusted using p.adjust in R using Bonferroni (# comparisons ≤ 10) or false discovery rate (# comparisons > 10) corrections. Statistical significance was ascribed to an alpha level of the adjusted *P*-values ≤ 0.05. Similarity between samples was assessed using the Yue–Clayton theta, which assesses the similarity between two samples based on (1) number of features in common between two samples, and (2) their relative abundances with $\theta = 0$ indicating totally dissimilar communities and $\theta = 1$ identical communities (*32*).

For functional experiments, mice were assigned randomly to groups. Mouse studies were not performed in a blinded fashion. Generally, each mouse of the different experimental groups is reported. Statistical significance was determined by ANOVA with multiple comparison correction (aov and TukeyHSD in R).

Table S1. Subject Tanner stage and disease severity for samples used in the study.

		Objective SCORAD			
Patient_ID	**Tanner**	**Baseline**	**Flare**	**Post-flare**	**Group**
AD01	2	-	45.1	4.6	
AD03	1	7	53.2	17.2	
AD04	2	4.2	42.1	6.2	More severe
AD06	2	-	36.6	15.3	
AD11	5	-	51.4	8.4	
AD02	1	10.7	22.1	11.2	
AD05	1	11.9	33.6	11.4	
AD07	1	13.2	34.2	18	Less severe
AD08	1	-	31.8	18.5	
AD09	1	-	29.4	13.1	
AD10	4	-	33.8	4.3	

Table S2. Clinical metadata for subjects in the study

	Atopic Dermatitis (AD) Patients	***AD - More Severe***	***AD - Less Severe***	**Healthy Controls (HC)**
Number of subjects	11	*5*	*6*	7
M:F	6:5	*2:3*	*4:2*	5:2
Age	7.6 ± 1.4	*10.4 ± 2.0*	*5.3 ± 1.4*	10.3 ± 0.8
Blood eosinophils, mean ± SE (normal 0.0-4.7%)*	9.5 ± 1.7	*11.5 ± 2.0*	*7.1 ± 2.6*	2.9 ± 0.7
Serum IgE, mean ± SE (normal 0.0-90.0 IU/mL)*	3206 ± 1618	*5515 ± 2526*	*318 ± 251*	49 ± 20
Asthma, ISAAC questionnaire (5)	4	*2*	*2*	0
Allergic rhinitis, ISAAC questionnaire (5)	11	*5*	*6*	1

*excludes AD08, AD09, HC07 due to subject declining blood draw

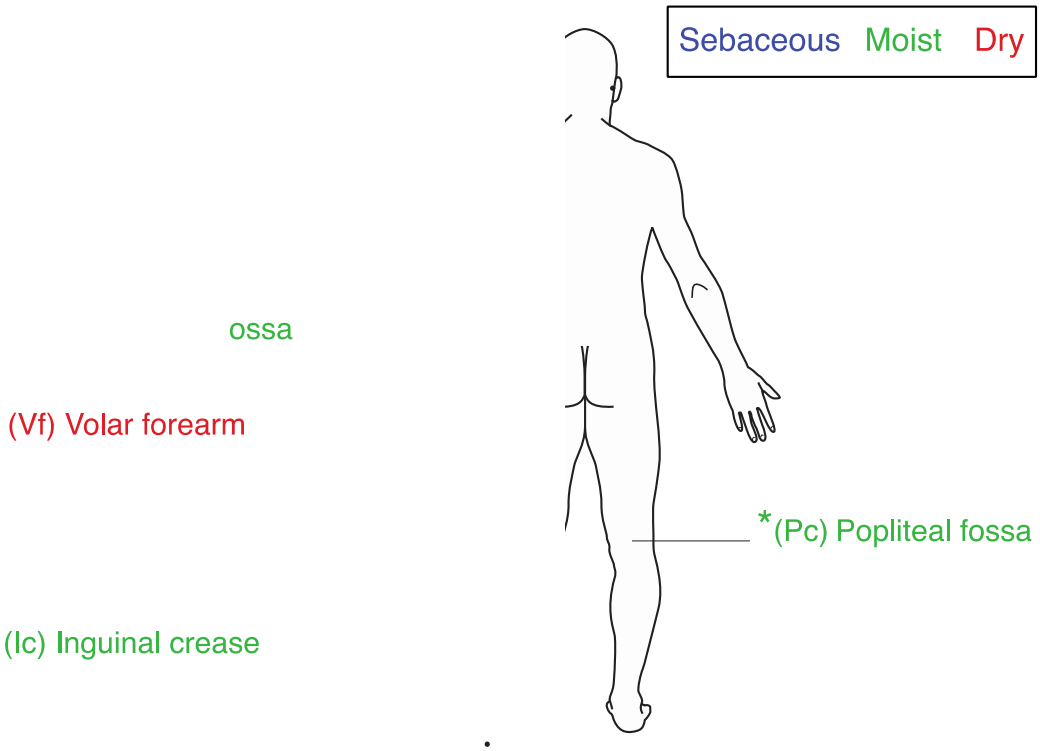

Fig. S1. Seven sites sampled bilaterally on AD patients and control children.

Sites colored by their microenvironment: sebaceous (blue), moist (green), and dry (red). Sites of AD disease predilection indicated with *.

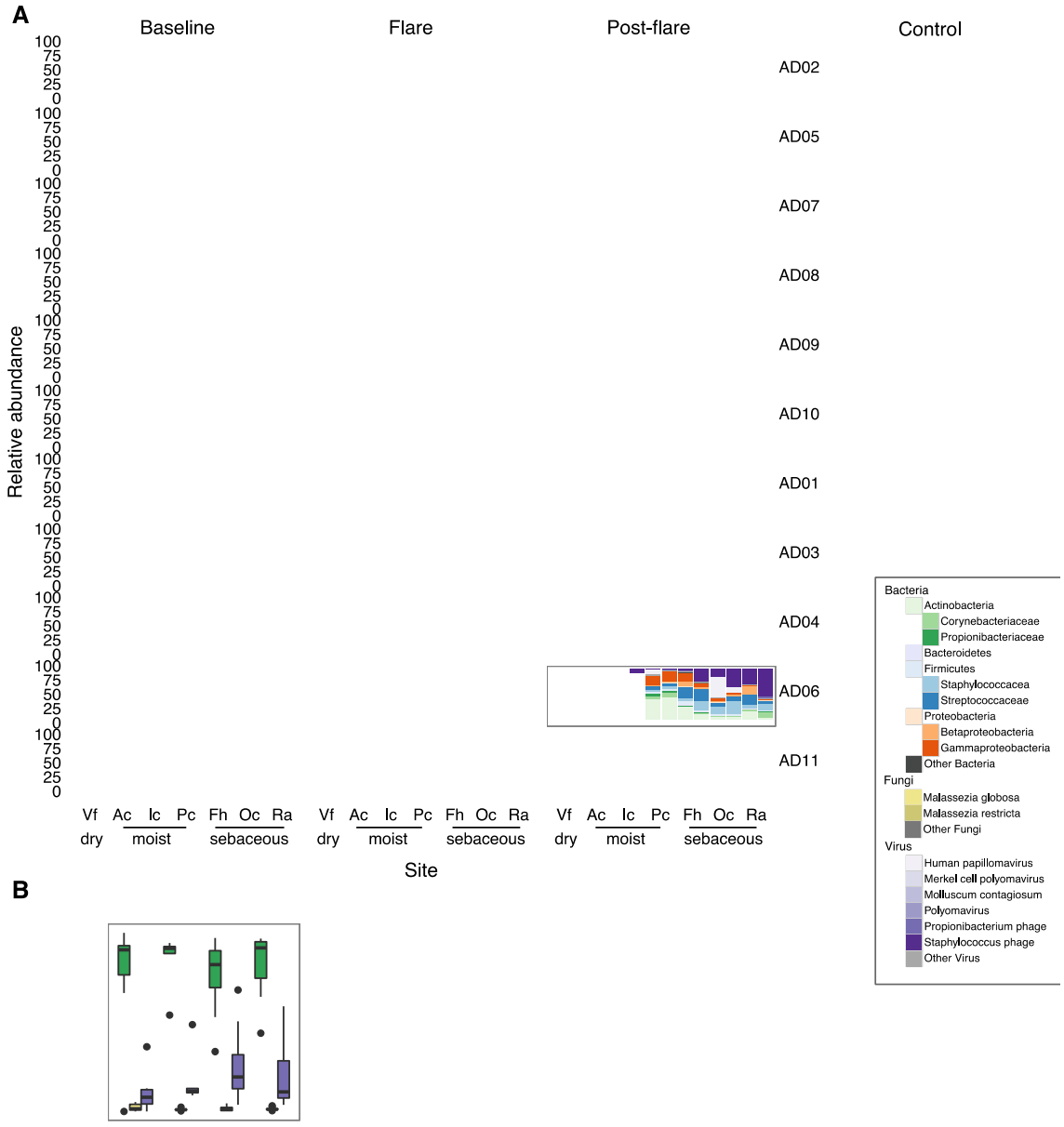

Fig. S2. Full multi-kingdom taxonomic classifications for AD patients and controls.

(**A**) Relative abundance of most abundant skin taxa for each super-kingdom for all sites in AD patients and controls. (**B**) Boxplots of mean relative abundance of different kingdoms by timepoint for the different site characteristics. Timepoints are Control (C), Baseline (B), Flare (F), and Post-flare (PF).

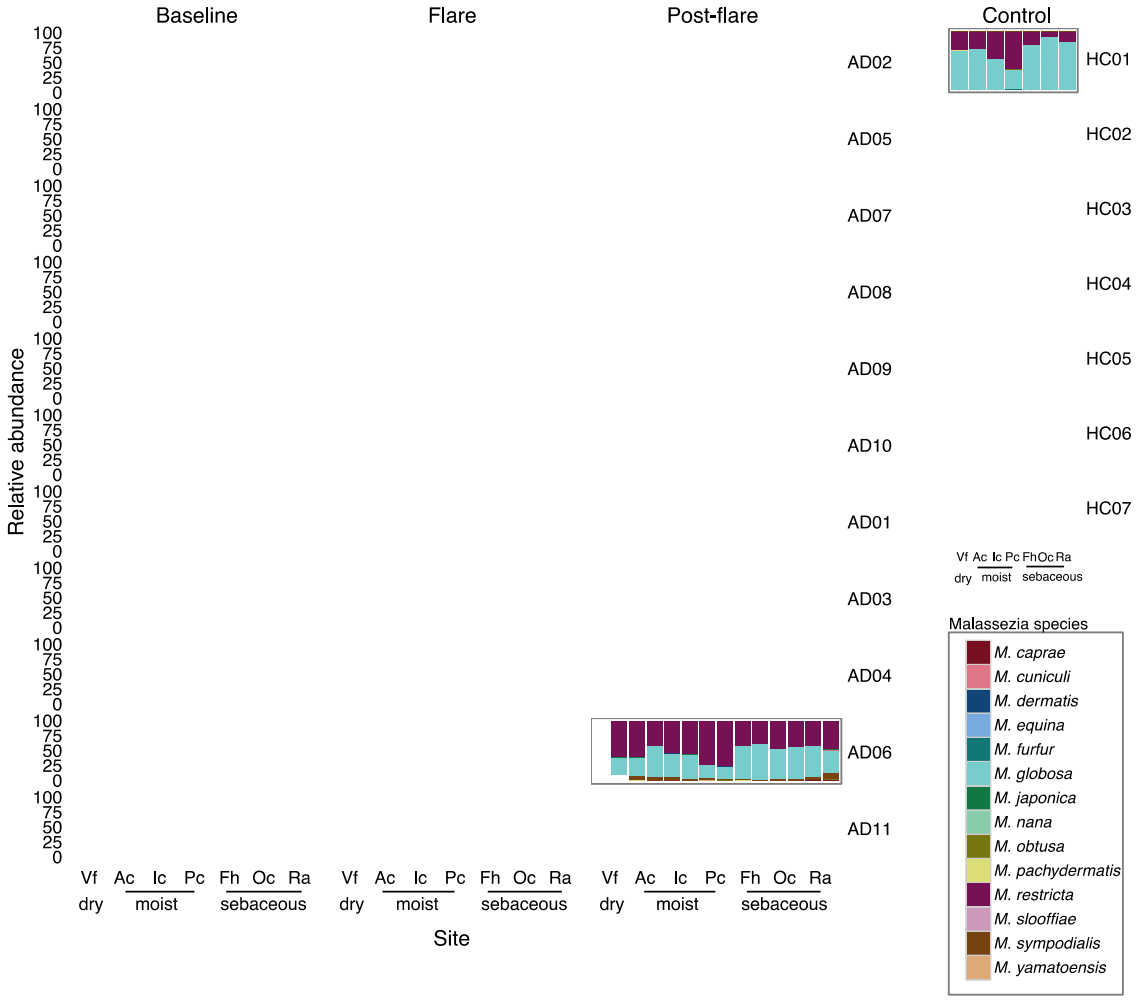

Fig. S3. Full Malassezia species classifications for AD patients and controls.

Relative abundance of Malassezia species for all sites in AD patients and controls.

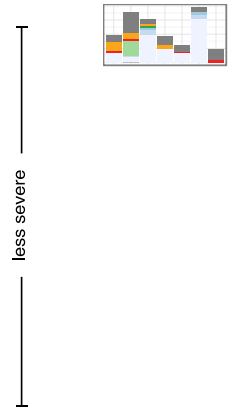

Fig. S4. Full eukaryotic virus classifications for AD patients and controls.

Relative abundance of eukaryotic viruses for all sites in AD patients and controls relative to the total microbial population.

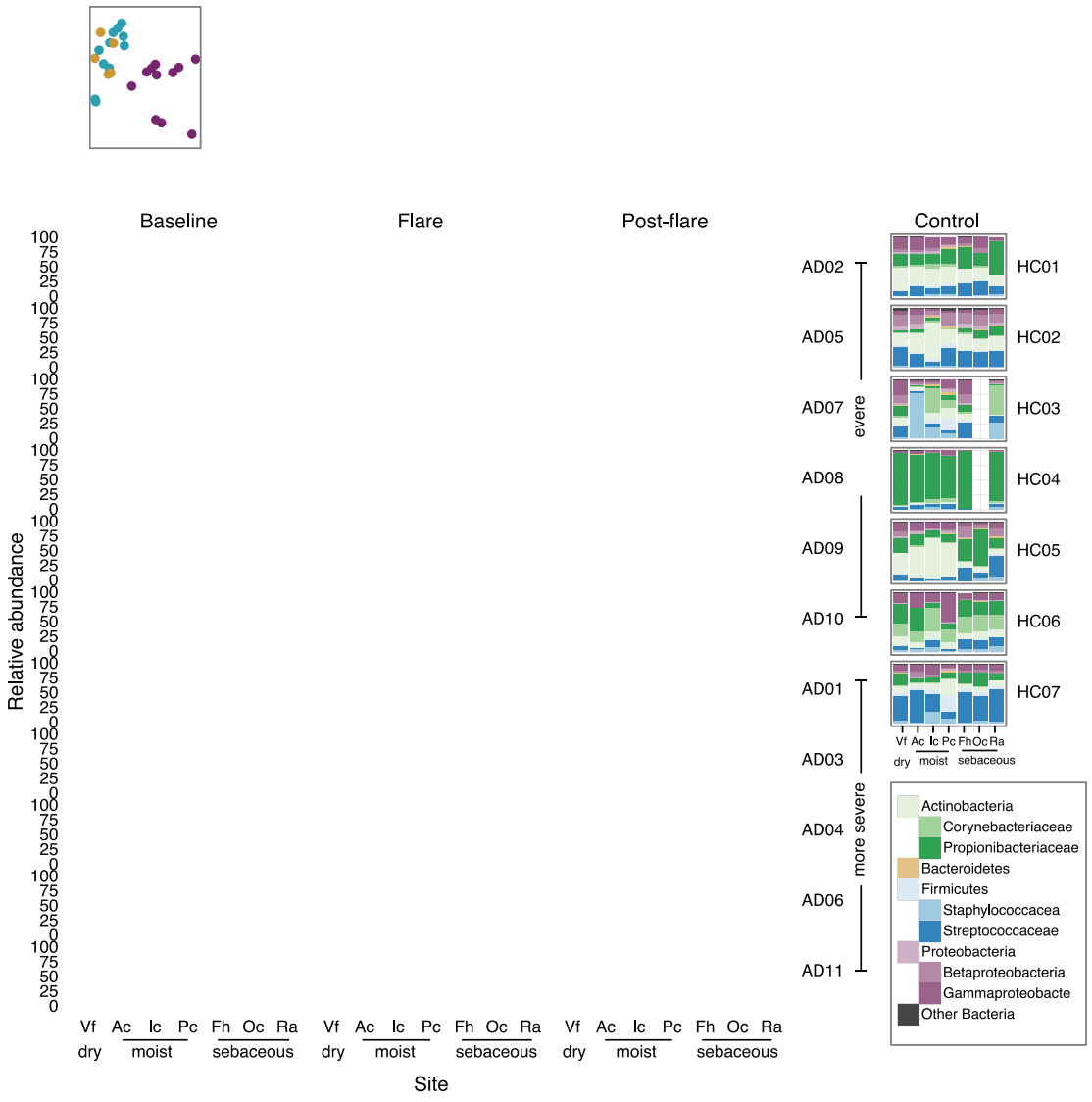

Fig. S5. Full bacterial taxonomic classifications for AD patients and controls.

(**A**) Shannon diversity versus objective SCORAD for all sites. Partial correlation (adjusting for disease state) with only significant correlations shown. (**B**) Relative abundance of bacterial genera for all sites in AD patients and controls. (**C**). Relative proportion of Staphylococcus versus objective SCORAD for all sites. Partial correlation (adjusting for disease state) with only significant correlations shown.

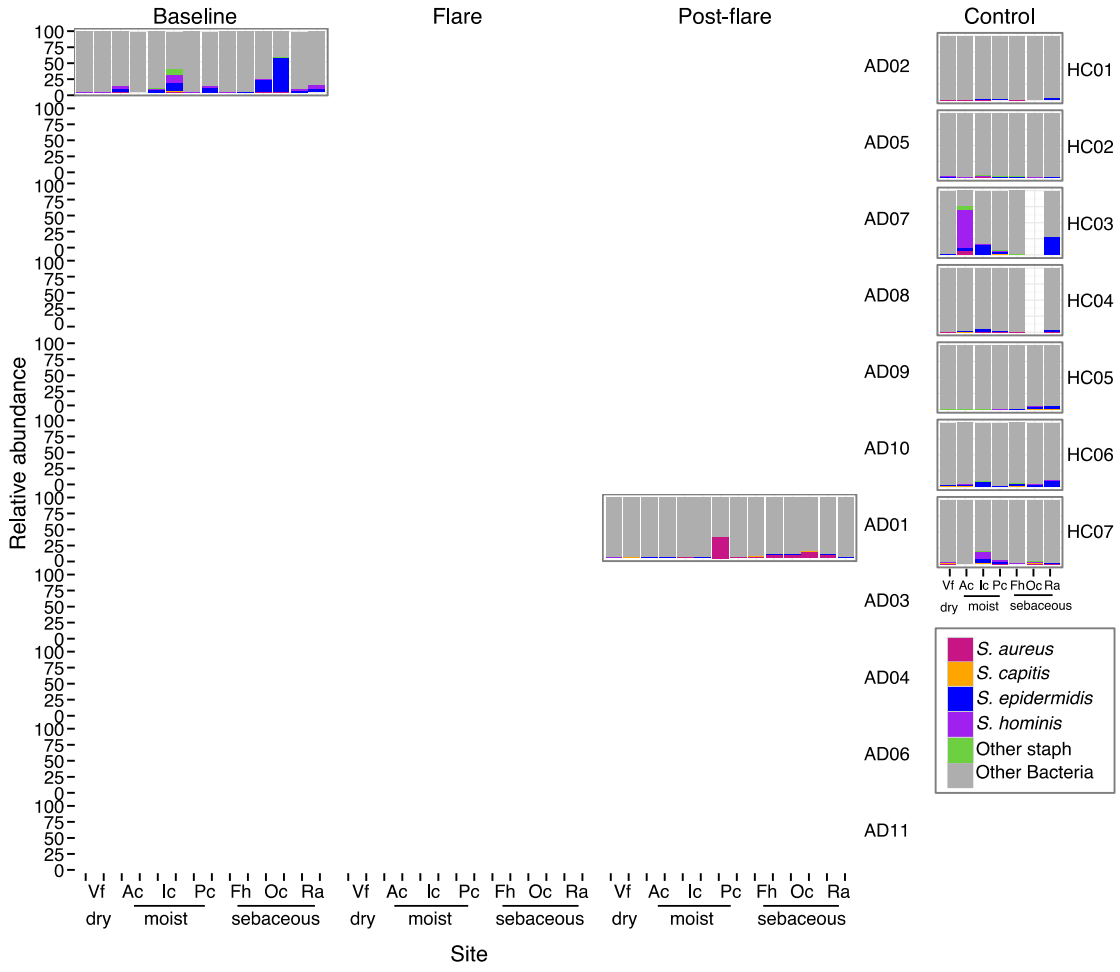

Fig. S6. Relative abundance of staphylococcal species in relation to total bacterial population for all sites in AD patients and controls.

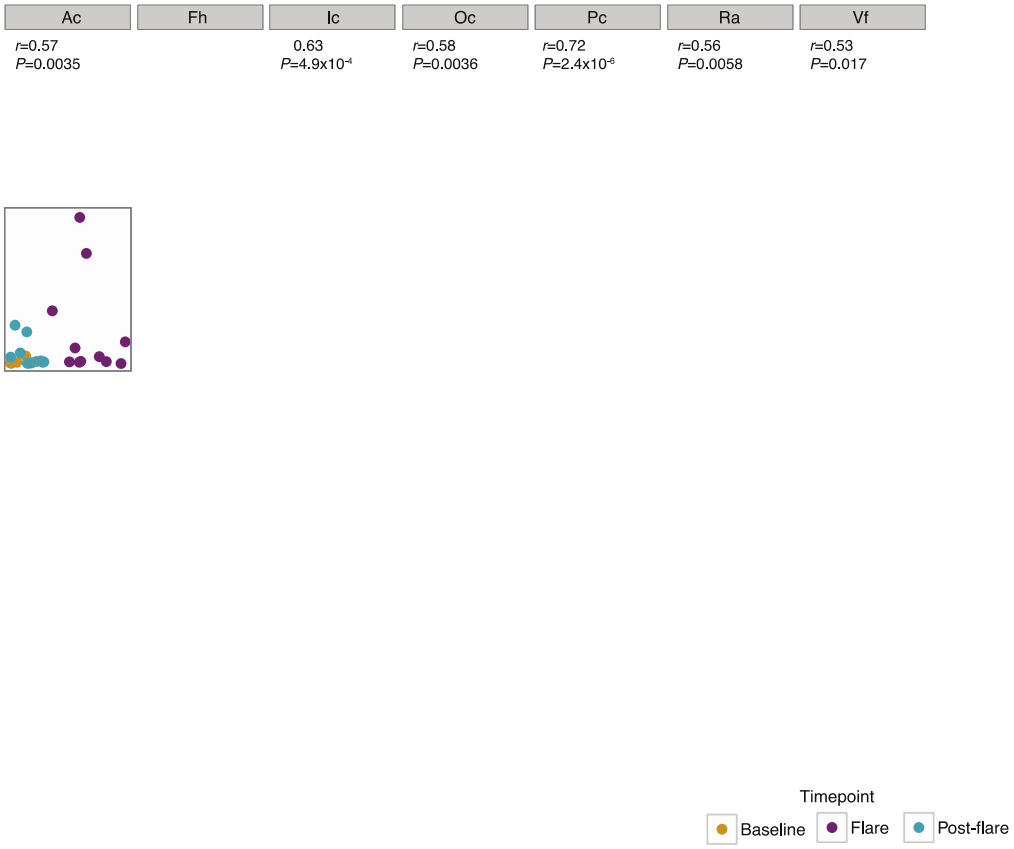

Fig. S7. Correlation of various staphylococcal species mean relative abundance and Obj SCORAD for all sites of patients.

Partial correlation (adjusting for disease state). Only significant correlations are indicated.

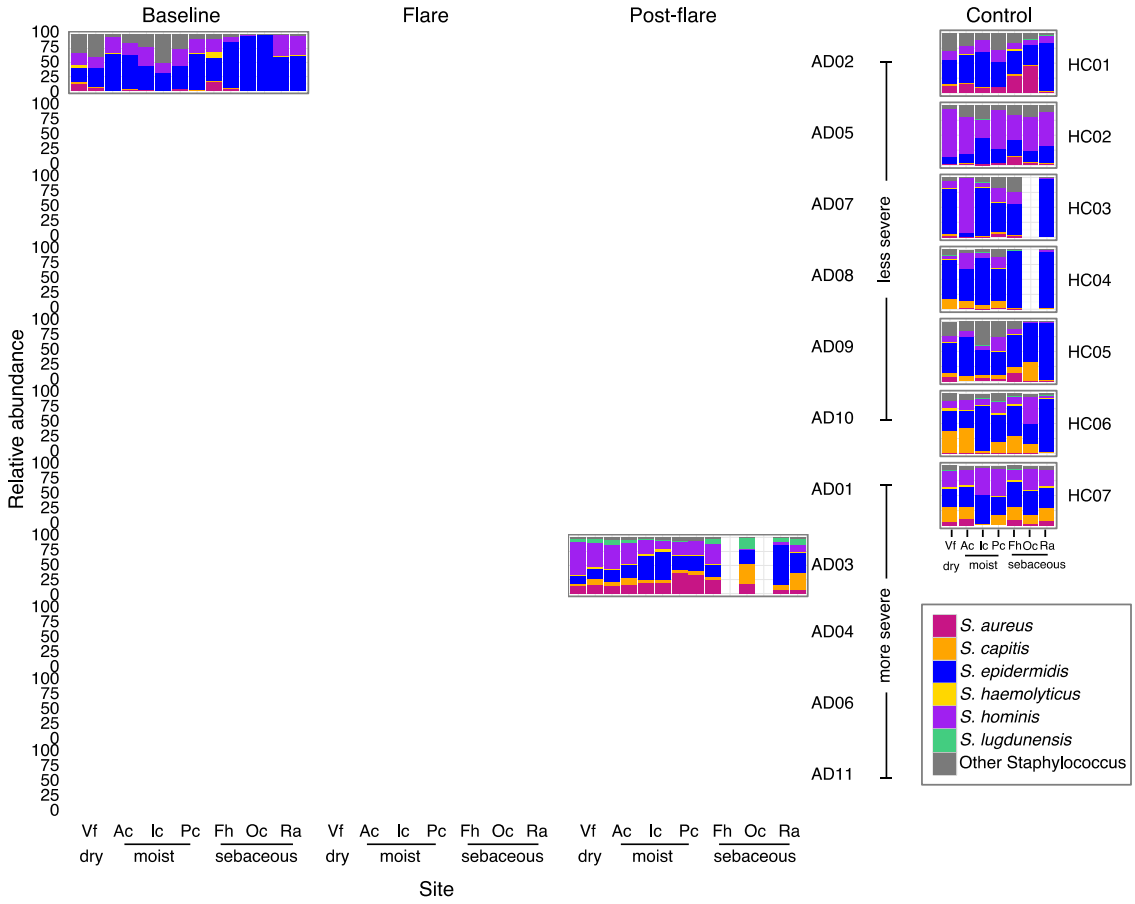

Fig. S8. Relative abundance of staphylococcal species for all sites in AD patients and controls.

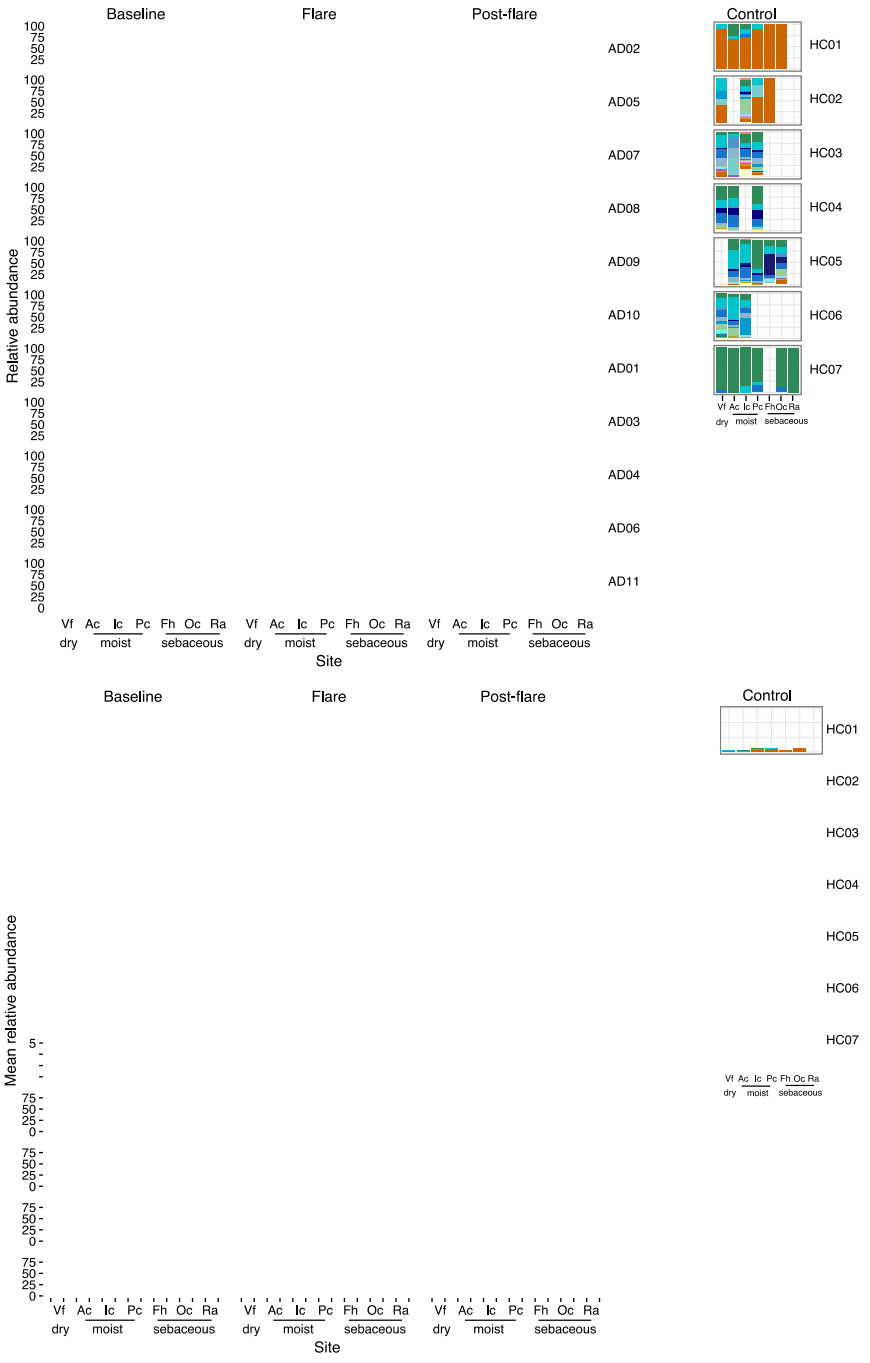

Fig. S9. *S. aureus* clades for AD patients and controls

(A) Cladogram of *S. aureus* strains based on SNVs in the core genome. Strains with names in red were isolated from patients in our study. Colors correspond to genomes of the same clade. Phylogenetically distant clade F1 is shown as an outgroup. (**B**) *S. aureus* clade relative abundances for all sites in AD patients and controls. Colors correspond to those in the (A). (C) *S. aureus* clade relative abundance normalized to percent *S. aureus* in the total bacterial population. Colors correspond to those in the (A).

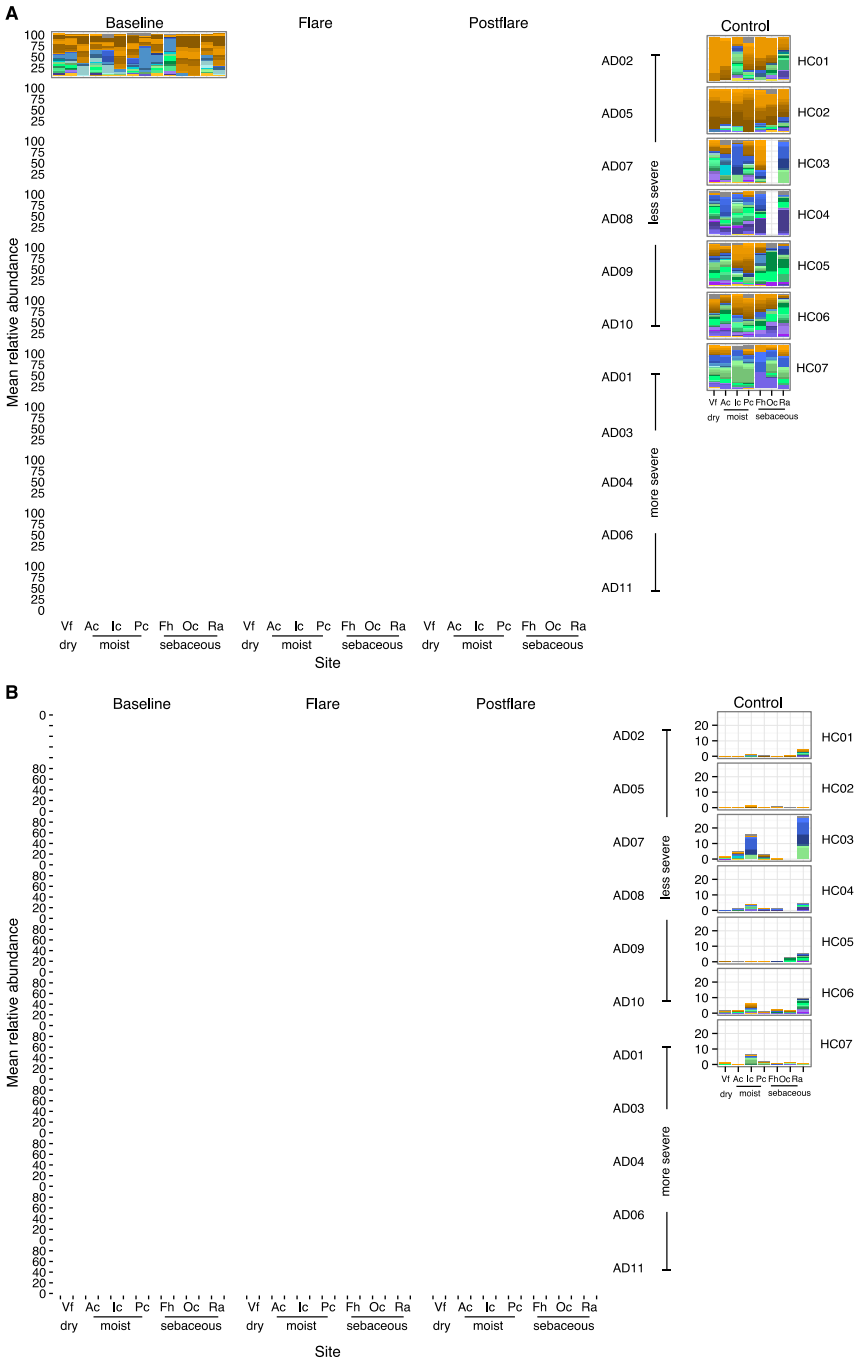

Fig. S10. *S. epidermidis* clades for AD patients and controls

(**A**) *S. epidermidis* clade relative abundances for all sites in AD patients and controls. Colors correspond to those in Figure 4A. (**B**) *S. epidermidis* clade relative abundance normalized to percent *S. epidermidis* in the total bacterial population. Colors correspond to those in Figure 4A.

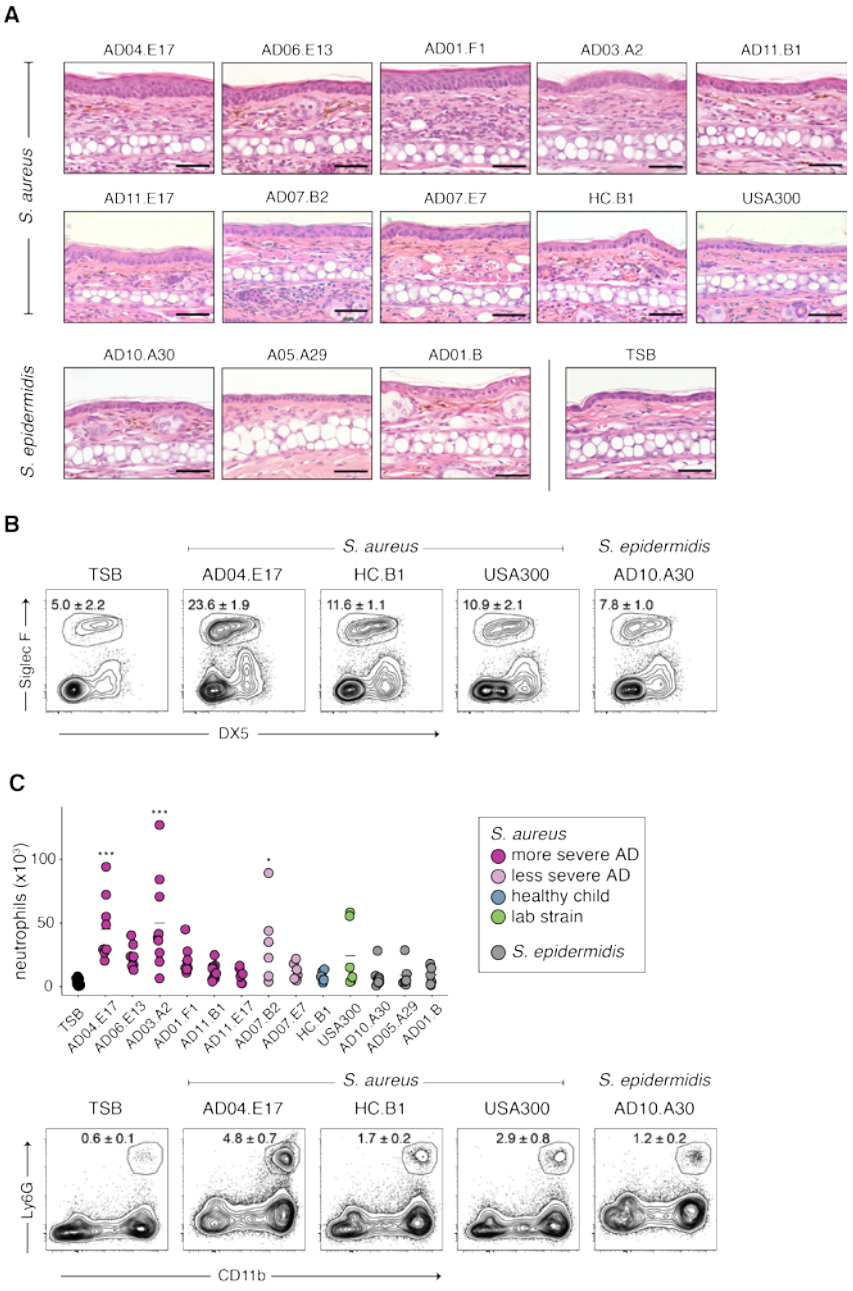

Fig. S11. Histologic and cutaneous innate immune cell responses with AD isolate association in a murine model.

(**A**) Representative histological images of the ear pinnae of mice associated with tryptic soy broth (TSB), and various AD patient *S. aureus* and *S. epidermidis* isolates. Scale bars, 50 μm. (**B**) **Representative FACS plots o**f mice in (Fig. 5D). (**C**) Absolute numbers and percentages of cutaneous neutrophils of mice. Color indicates origin and species of the isolate. Results are cumulative data from 2 or 3 independent experiments, 3 mice per group. *P<0.05, **P<0.01, ***P<0.001 as calculated by ANOVA with multiple comparison correction.

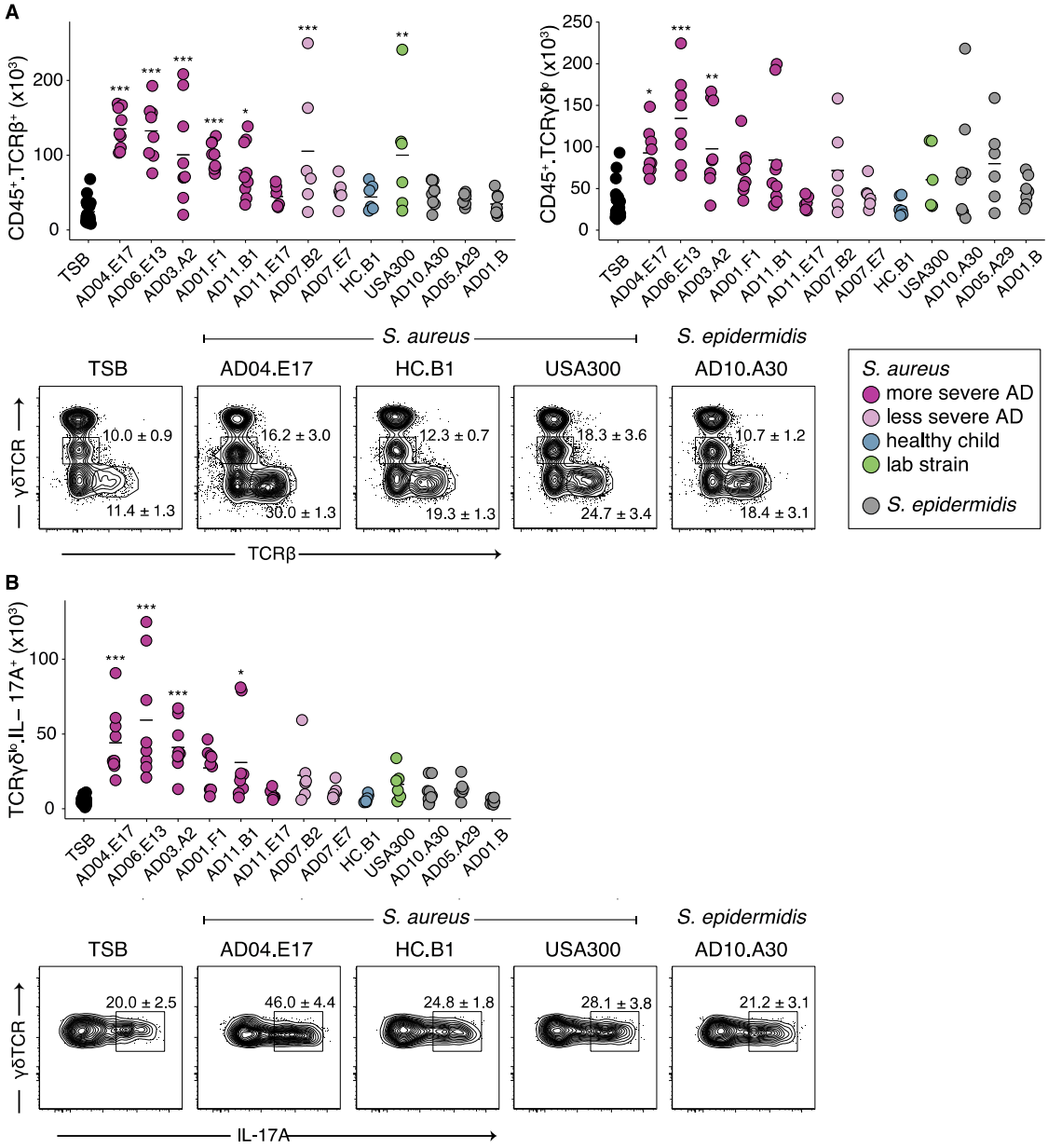

Fig. S12. CD45$^+$ cutaneous immune responses with AD isolate association in a murine model.

(**A**) Absolute numbers and representative flow plots of skin CD45$^+$ γδ^{low} and TCRβ$^+$ cells with topical application of TSB and various AD patient *S. aureus* and *S. epidermidis* isolates. (**B**) Absolute numbers and percentages of IL-17A$^+$ γδ^{low} T cells. Results are representative of 2 or 3 independent experiments. *P<0.05, **P<0.01, ***P<0.001 as calculated by ANOVA with multiple comparison correction.

References

1. H. C. Williams, P. G. Burney, A. C. Pembroke, R. J. Hay, The U.K. Working Party's Diagnostic Criteria for Atopic Dermatitis. III. Independent hospital validation. *The British journal of dermatology* **131**, 406-416 (1994).
2. H. C. Williams, P. G. Burney, D. Strachan, R. J. Hay, The U.K. Working Party's Diagnostic Criteria for Atopic Dermatitis. II. Observer variation of clinical diagnosis and signs of atopic dermatitis. *The British journal of dermatology* **131**, 397-405 (1994).
3. B. Kunz *et al.*, Clinical validation and guidelines for the SCORAD index: consensus report of the European Task Force on Atopic Dermatitis. *Dermatology* **195**, 10-19 (1997).
4. A. P. Oranje, E. J. Glazenburg, A. Wolkerstorfer, F. B. de Waard-van der Spek, Practical issues on interpretation of scoring atopic dermatitis: the SCORAD index, objective SCORAD and the three-item severity score. *The British journal of dermatology* **157**, 645-648 (2007).
5. M. I. Asher *et al.*, International Study of Asthma and Allergies in Childhood (ISAAC): rationale and methods. *The European respiratory journal* **8**, 483-491 (1995).
6. H. H. Kong *et al.*, Temporal shifts in the skin microbiome associated with disease flares and treatment in children with atopic dermatitis. *Genome research* **22**, 850-859 (2012).
7. J. Oh *et al.*, Biogeography and individuality shape function in the human skin metagenome. *Nature* **514**, 59-64 (2014).
8. J. K. Teer *et al.*, Systematic comparison of three genomic enrichment methods for massively parallel DNA sequencing. *Genome research* **20**, 1420-1431 (2010).
9. B. Langmead, S. L. Salzberg, Fast gapped-read alignment with Bowtie 2. *Nature methods* **9**, 357-359 (2012).
10. O. E. Francis *et al.*, Pathoscope: species identification and strain attribution with unassembled sequencing data. *Genome research* **23**, 1721-1729 (2013).
11. A. R. Quinlan, I. M. Hall, BEDTools: a flexible suite of utilities for comparing genomic features. *Bioinformatics* **26**, 841-842 (2010).
12. A. L. Delcher, A. Phillippy, J. Carlton, S. L. Salzberg, Fast algorithms for large-scale genome alignment and comparison. *Nucleic acids research* **30**, 2478-2483 (2002).
13. S. Noda *et al.*, The Asian atopic dermatitis phenotype combines features of atopic dermatitis and psoriasis with increased TH17 polarization. *The Journal of allergy and clinical immunology* **136**, 1254-1264 (2015).
14. J. Oh *et al.*, Temporal stability of the human skin microbiome. *Cell* **165**, 854-866 (2016).
15. A. McKenna *et al.*, The Genome Analysis Toolkit: a MapReduce framework for analyzing next-generation DNA sequencing data. *Genome research* **20**, 1297-1303 (2010).
16. T. D. Lieberman *et al.*, Genetic variation of a bacterial pathogen within individuals with cystic fibrosis provides a record of selective pressures. *Nature genetics* **46**, 82-87 (2014).

17. K. Zhang *et al.*, New quadriplex PCR assay for detection of methicillin and mupirocin resistance and simultaneous discrimination of Staphylococcus aureus from coagulase-negative staphylococci. *Journal of clinical microbiology* **42**, 4947-4955 (2004).
18. F. Martineau, F. J. Picard, P. H. Roy, M. Ouellette, M. G. Bergeron, Species-specific and ubiquitous DNA-based assays for rapid identification of Staphylococcus epidermidis. *Journal of clinical microbiology* **34**, 2888-2893 (1996).
19. A. V. Zimin *et al.*, The MaSuRCA genome assembler. *Bioinformatics* **29**, 2669-2677 (2013).
20. A. Bankevich *et al.*, SPAdes: a new genome assembly algorithm and its applications to single-cell sequencing. *Journal of computational biology : a journal of computational molecular cell biology* **19**, 455-477 (2012).
21. B. J. Walker *et al.*, Pilon: An Integrated Tool for Comprehensive Microbial Variant Detection and Genome Assembly Improvement. *PloS one* **9**, (2014).
22. R. Chikhi, P. Medvedev, Informed and automated k-mer size selection for genome assembly. *Bioinformatics* **30**, 31-37 (2014).
23. K. Galens *et al.*, The IGS Standard Operating Procedure for Automated Prokaryotic Annotation. *Standards in genomic sciences* **4**, 244-251 (2011).
24. CLSI, "Performance standards for antimicrobial susceptibility testing. CLSI approved standard M100-S23.," (Clinical and Laboratory Standards Institute, Wayne, PA., 2013).
25. R. C. Edgar, Search and clustering orders of magnitude faster than BLAST. *Bioinformatics* **26**, 2460-2461 (2010).
26. T. Lefebure, M. J. Stanhope, Evolution of the core and pan-genome of Streptococcus: positive selection, recombination, and genome composition. *Genome biology* **8**, R71 (2007).
27. R. Schmieder, R. Edwards, Quality control and preprocessing of metagenomic datasets. *Bioinformatics* **27**, 863-864 (2011).
28. P. Bardou, J. Mariette, F. Escudie, C. Djemiel, C. Klopp, jvenn: an interactive Venn diagram viewer. *BMC bioinformatics* **15**, 293 (2014).
29. S. Naik *et al.*, Commensal-dendritic-cell interaction specifies a unique protective skin immune signature. *Nature* **520**, 104-108 (2015).
30. S. Naik *et al.*, Compartmentalized control of skin immunity by resident commensals. *Science* **337**, 1115-1119 (2012).
31. H. Wickham, ggplot2: Elegant Graphics for Data Analysis. *Use R*, 1-212 (2009).
32. J. C. Yue, M. K. Clayton, A similarity measure based on species proportions. *Commun Stat-Theor M* **34**, 2123-2131 (2005).